Supporting Information

Segmentally Structured Disk Triboelectric Nanogenerator for Harvesting Rotational Mechanical Energy

Long Lin,[†,§] Sihong Wang,[†,§] Yannan Xie,[†] Qingshen Jing,[†] Simiao Niu,[†] Youfan Hu,[†] and Zhong Lin Wang[†,‡,*]

†School of Materials Science and Engineering, Georgia Institute of Technology, Atlanta, Georgia 30332-0245

[‡]Beijing Institute of Nanoenergy and Nanosystems, Chinese Academy of Sciences, Beijing, China

[*]Address correspondence to zlwang@gatech.edu

[§]These authors contributed equally to this work

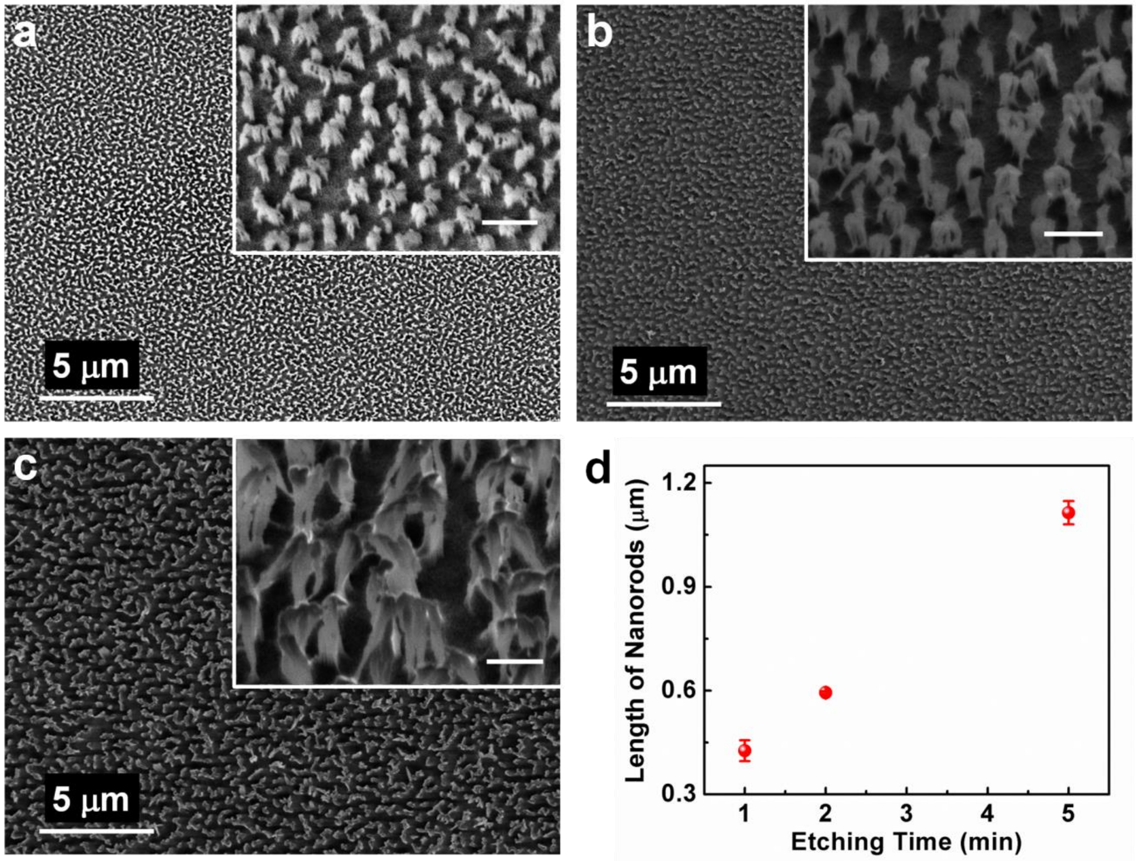

Figure S1. Analysis of the morphology of the Kapton nanorods (NRs) with variable etching times. (a) The top-view scanning electron microscopy (SEM) image for the Kapton NRs after 1 minute etching. The inset is a 30˚-tilted view high magnification SEM image. The scale bar is 500 nm. (b) The top-view SEM image for the Kapton NRs after 2 minute etching. The inset is a 30˚-tilted view high magnification SEM image. The scale bar is 500 nm. (c) The top-view SEM image for the Kapton NRs after 5 minute etching. The inset is a 30˚-tilted view high magnification SEM image. The scale bar is 500 nm. (d) Summary of the relationship between the average lengths of the etched NRs and the etching time.

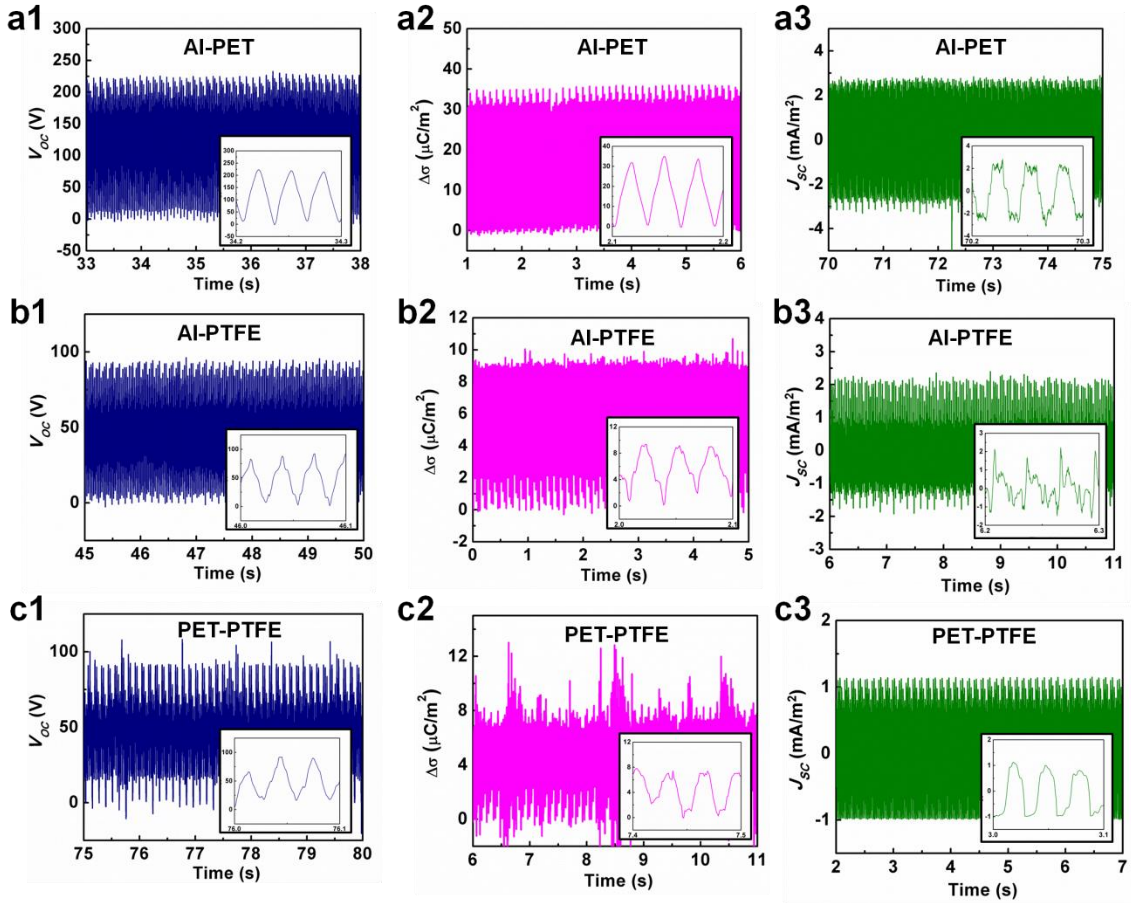

Figure S2. The measurement of output performance for other material systems. (a1-a3) The measured (a1) open-circuit voltage, (a2) transferred charge density, and (a3) short-circuit current density for the Al-polyethylene terephthalate (PET) system. The insets show the enlarged output profiles in three cycles. (b1-b3) The measured (b1) open-circuit voltage, (b2) transferred charge density, and (b3) short-circuit current density for the Al-polytetrafluoroethylene (PTFE) system. The insets show the enlarged output profiles in three cycles. (c1-c3) The measured (c1) open-circuit voltage, (c2) transferred charge density, and (c3) short-circuit current density for the PET-PTFE system. The insets show the enlarged output profiles in three cycles. All the measurements were carried out at 500 rpm with Configuration 3.

Table S1. Frequency analysis of the output with different configurations.

Configuration	**1**	**2**	**3**
$f_{voltage}$ **(Hz)**	**1.64**	**3.97**	**6.68**
f_{charge} **(Hz)**	**1.65**	**3.40**	**7.19**
$f_{current}$ **(Hz)**	**1.70**	**3.39**	**6.41**
$f_{theoretical}$ **(Hz)**	**1.67**	**3.33**	**6.67**

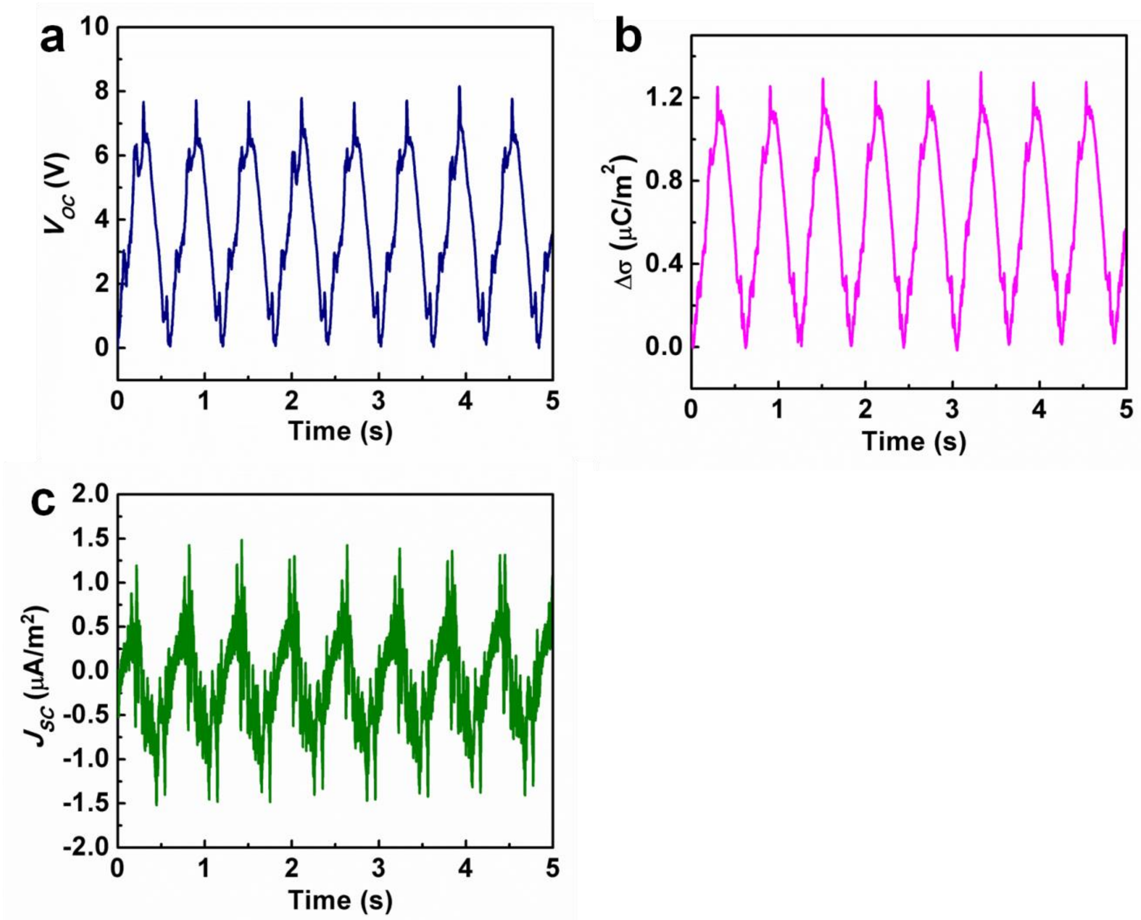

Figure S3. Control experiment using the full-round-shape configuration of Al foil and Kapton film. The measurement was carried output by rotating the Al part on the Kapton part at 100 rpm with intimate contact. (a-c) The measured (a) open-circuit voltage, (b) transferred charge density, and (c) short-circuit current density for the control experiment. The much lower output compared to the other configurations confirms that the in-plane charge separation by tailoring the Al foil and Kapton film into specific shape is required for high output, indicating the validity of the proposed theory for the working principle of the disk TENG.

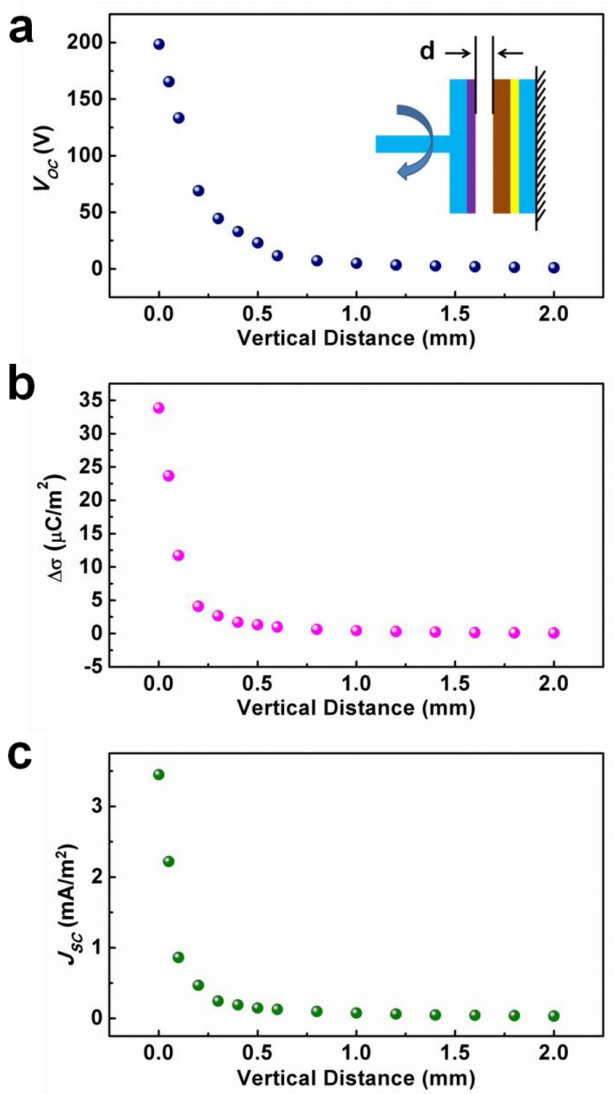

Figure S4. The dependence of the measured output performance of the disk TENG on the vertical distance between the two plates. (a) The measured open-circuit voltage with variable vertical distances. The inset is the schematic illustration showing the design of this measurement, and d indicates the vertical distance. (b) The measured transferred charge density with variable vertical distances. (c) The measured short-circuit current density with variable vertical distances. All the measurements were carried out with Configuration 1 at 100 rpm.

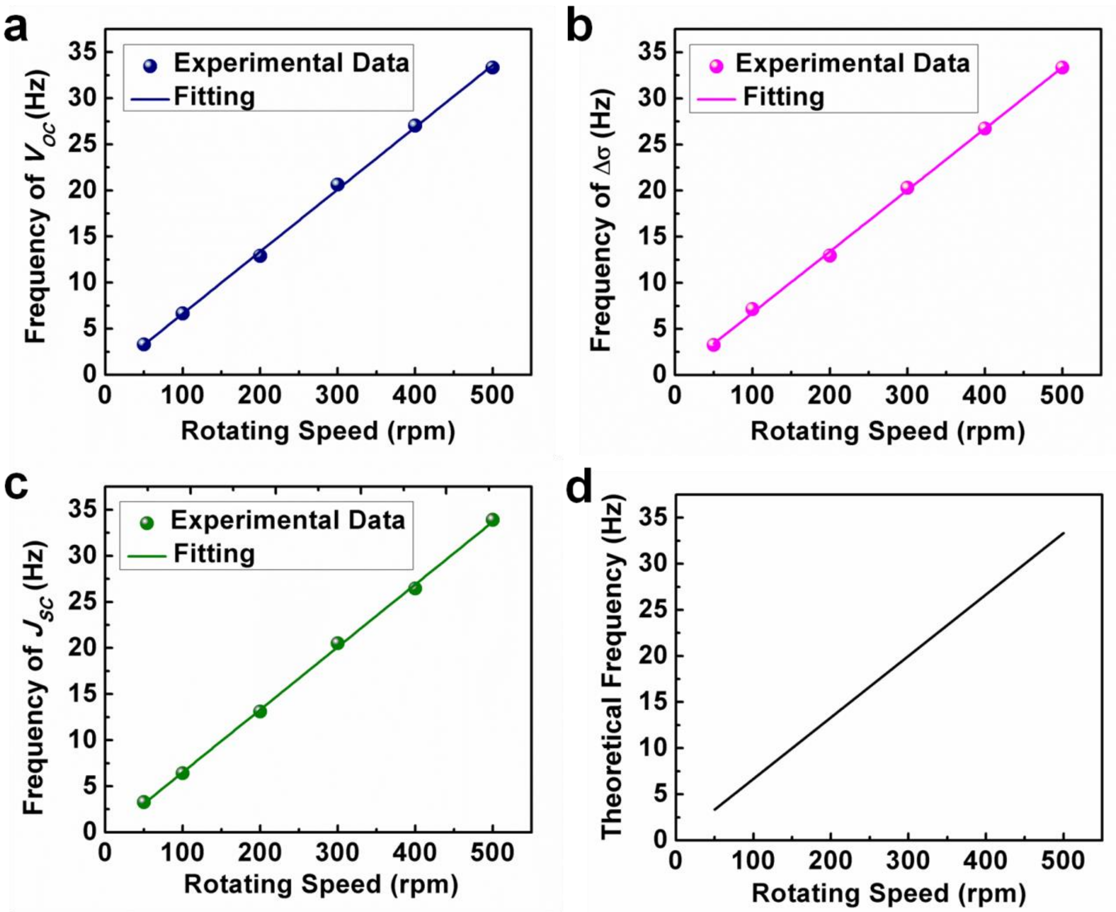

Figure S5. The frequency of the measured output signals with variable rotating speeds. (a-c) The frequency of the measured (a) open-circuit voltage, (b) transferred charge density, and (c) short-circuit current density with variable rotating speeds ranging from 50 to 500 rpm. (d) The theoretically calculated frequency of the cyclic output with variable rotating speeds. The linear relationship between the frequencies of the output signals and the rotating speed, as well as their excellent agreement with theoretically calculated values implies that the disk TENG could serve as a reliable self-powered angular speed sensor with simple frequency analysis.

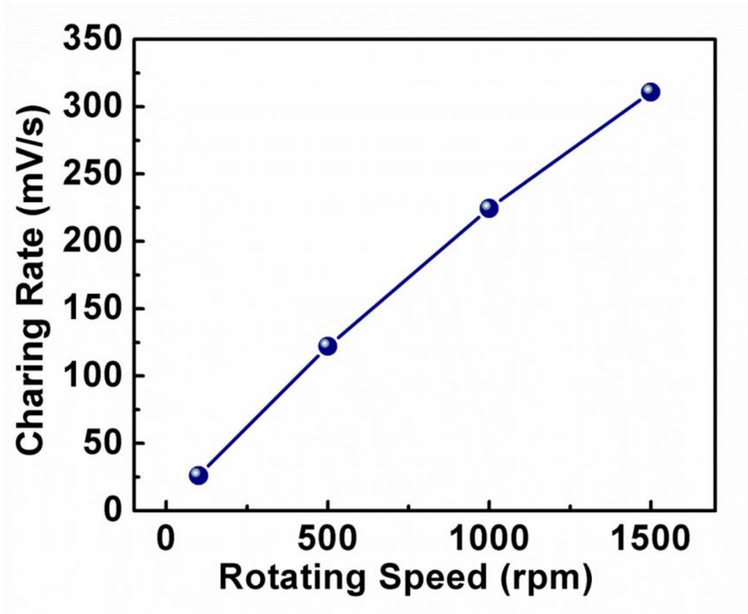

Figure S6. The charging rates of a 22 μF capacitor charged by the disk TENG with Configuration 3 at variable speeds from 100 to 1500 rpm.

Videos

Video S1. The constant powering of 60 green light emitting diodes by the disk TENG.

Video S2. The powering of 60 green light emitting diodes by the disk TENG, from low frequency to high frequency.